Statistical optimization of phytol and polyunsaturated fatty acid production in the Antarctic microalga *Micractinium variabile* KSF0031

Eun Jae Kim[1], Hyunsik Chae[1], Man Hyung Koo[2], Jihyeon Yu[1], Hyunjoong Kim[1,3], Sung Mi Cho[1,4], Kwang Won Hong[5], Joo Young Lee[5], Ui Joung Youn[1,4], Sanghee Kim[1], Han-Gu Choi[1] and Se Jong Han[1,4,*]

[1]*Division of Life Sciences, Korea Polar Research Institute, Incheon 21990, Korea*
[2]*Research Unit of Cryogenic Novel Material, Korea Polar Research Institute, Incheon 21990, Korea*
[3]*Department of Systems Biology, Institute of Life Science and Biotechnology, Yonsei University, Seoul 03722, Korea*
[4]*Department of Polar Sciences, University of Science and Technology, Incheon 21990, Korea*
[5]*R&D Department, Microalgae Ask Us Co., Ltd., Gangneung 25451, Korea*

Polar microorganisms produce physiologically active substances to adapt to harsh environments, and these substances can be used as biomedical compounds. The green microalga *Micractinium variabile* KSF0031, which was isolated from Antarctica, produced phytol, a natural antimicrobial agent. Furthermore, several polyunsaturated fatty acids (PUFAs), including omega-3, exhibit antioxidant properties. Here statistical methods (Plackett-Burman design and Box-Behnken design) were used to optimize the culture medium of KSF0031 to improve biomass production, and K_2HPO_4, $MgSO_4 \cdot 7H_2O$, and ammonium ferric citrate green (AFCg) were selected as significant components of the culture medium. Changes in the concentration of K_2HPO_4 and $MgSO_4 \cdot 7H_2O$ as positive factors and AFCg as a negative factor affected cell growth to a remarkable degree. The biomass production in a 100 L culture using the optimized medium for 24 d at 18°C was improved by 37.5% compared to that obtained using the original BG-11 medium. The quantities of PUFAs and phytol obtained were 13 mg g^{-1} dry cell weight (DCW) and 10.98 mg g^{-1} DCW, which represent improved yields of 11.70% and 48.78%, respectively. The results of this study could contribute to an improved production of phytol and fatty acids from Antarctic microalgae in the biomedical industry.

Keywords: Antarctic algae; growth medium optimization; *Micractinium variabile*; phytol; polyunsaturated fatty acids

Abbreviations: AFCg, ammonium ferric citrate green; DHA, docosahexaenoic acid; EPA, eicosapentaenoic acid; FAMEs, fatty acid methyl esters; PUFAs, polyunsaturated fatty acids

INTRODUCTION

The Antarctic and Arctic are polar regions with a year-round cold climate. Antarctica exhibits some of the coldest temperatures on earth because the supply of warm heat is interrupted by strong winds and the Antarctic circumpolar current (Barker et al. 2007). Psychrotrophic and psychrophilic microorganisms, which are adapted

to cold environments, produce various physiologically active substances, such as cold-active enzymes and ice-binding proteins (Borchert et al. 2017, Brouchkov et al. 2017, Kim et al. 2017, Park et al. 2018). Polar microalgae also have mechanisms to survive in low-temperature environments. In a recent study, a novel ice-binding protein derived from polar microalgae was reported (Cho et al. 2019). Moreover, to survive at low temperatures, polar microalgae accumulate polyunsaturated fatty acids (PUFAs) inside their cells, which increase membrane fluidity; the flexible cell membrane reduces physical damage caused by the growth of ice crystals (Teoh et al. 2004). Unsaturated fatty acids have lower melting points than saturated fatty acids. This is due to their chemical structure, which includes multiple double bonds (Siram et al. 2019). PUFAs are valuable compounds, which include linoleic acid, gamma-linolenic acid, eicosapentaenoic acid (EPA), and docosahexaenoic acid (DHA). EPA and DHA, representative omega-3 unsaturated fatty acids, are essential for maintaining health (Gutiérrez et al. 2019). The PUFAs of polar microalgae, can be used as food additives and nutrients (Kim et al. 2016, Remize et al. 2021). In addition, ethanol extracts from the Antarctic freshwater microalgae *Chloromonas reticulata* KSF0100 and *Microactinium* sp. KSF0105 have been reported to exhibit anticancer and anti-inflammatory activities (Suh et al. 2018, 2019).

Phytol is a member of the diterpene alcohol family and a precursor of vitamins E and K1. Phytol is a component of chlorophyll, which is produced by all photosynthetic organisms, such as green algae, other plants, and some bacteria. Phytol has been reported to show anticancer activity, immunity enhancement, and antimicrobial effect (Komiya et al. 1999, Prabuseenivasan et al. 2006, Chowdhury et al. 2013, Murbach Teles Andrade et al. 2014). Phytol exhibits antibacterial and antifungal activities, high stability, and low toxicity; therefore, it is useful as a surface disinfectant (Ghaneian et al. 2015). Chemical synthesis is the primary method of industrial-scale phytol production; however, it is expensive and causes environmental pollution (Islam et al. 2015). The production of biopharmaceuticals, such as phytol, using microalgae could be an environment-friendly and sustainable method that could lower the production costs while reducing greenhouse gases, as it utilizes sunlight and atmospheric CO_2 (Khan et al. 2018). In this study, we report, for the first time, that *Microactinium variabile* KSF0031, a species recently discovered in the Antarctic (Chae et al. 2019), accumulates significant quantities of phytol and PUFAs. Here, we optimized its medium to improve the production of cell biomass and bioactive ingredients.

MATERIALS AND METHODS

Strain and culture media

The Antarctic freshwater microalga *Microactinium variabile* KSF0031 was isolated from Ardley Island, South Shetland Islands, Antarctica (Chae et al. 2019). The culture was maintained in BG-11 medium (Stanier et al. 1971). The BG-11 medium contained the following (mM): $NaNO_3$, 17.60; K_2HPO_4, 0.23; $MgSO_4 \cdot 7H_2O$, 0.30; $CaCl_2 \cdot 2H_2O$, 0.24; citric acid, 0.031; ammonium ferric citrate green (AFCg), 0.021; $EDTA \cdot Na_2$, 0.0027; Na_2CO_3, 0.19; trace metals, 0.058 (H_3BO_3, 0.046; $MnCl_2 \cdot 4H_2O$, 0.009; $ZnSO_4 \cdot 7H_2O$, 0.077; $Na_2MoO_4 \cdot 2H_2O$, 0.0016; $CuSO_4 \cdot 5H_2O$, 0.0003; $Co(NO_3)_2 \cdot 6H_2O$, 0.00017).

Culture conditions

Ten liters of seed with approximately 5×10^5 cells mL^{-1} was inoculated in 100 L of BG-11 medium at 18°C (Supplementary Fig. S1) and cultured for 24 d. The KSF0031 was irradiated with cool white fluorescent light (80 μmol photon m^{-2} s^{-1}) on a 16 : 8 h light-dark cycle with filtered atmospheric air supplied at a rate of 5 L min^{-1}.

Statistical optimization

The essential components for the growth of KSF0031 were analyzed using the Plackett-Burman design (Plackett and Burman 1946). A classic way to screen for large variables is to use the Plackett-Burman design, which is programmed to identify critical parameters using n + 1 experiments (Ekpenyong et al. 2017). Based on these results, five elements of the BG-11 medium were selected and represented at two levels, low (-) and high (+) concentrations, producing a first-order model. The effect of each factor on cell numbers was calculated using Eq. (1):

$$Y = \beta_0 + \Sigma \beta_i X_i \qquad (1)$$

, where Y denotes the response (number of cells), β_0 is the model intercept, β_i is the linear factor coefficient, and X_i is the level of each variable. The concentrations of the medium components were optimized using the Box-Behnken surface response method (Box and Behnken 1960). The Box-Behnken design was devised for analyses where each factor varies among the three levels (-1, 0, +1) (Czyrski and Sznura 2019). Accordingly, the individual factors in this study were coded into three disparate levels: (-) for low, (0) for intermediate, and (+) for high concentrations.

A second-order polynomial model was designed to investigate the influence of individual components on the predicted response. A second-order polynomial model was calculated using Eq. (2):

$$Y = \beta_0 + \Sigma\beta_i X_i + \Sigma\beta_{ij} X_i X_j + \Sigma\beta_{ii} X_i^2 \qquad (2)$$

, where Y denotes the predicted response (number of cells), β_0 is the constant coefficient, β_i, β_{ij}, and β_{ii} denote the regression coefficients of the model, and X_i and X_j represent the coded values of independent nutrient variables.

Cell growth monitoring and assay of fatty acid methyl esters and phytol

The growth of KSF0031 was analyzed by counting the cells using a hemocytometer and an optical microscope (Zeiss Axio Imager A2, Gottingen, Germany). Twenty milligrams of freeze-dried KSF0031 samples was used to extract fatty acids and phytol. Fatty acid methyl esters (FAMEs) were converted from crude lipids and analyzed as described previously (Kim et al. 2016). FAMEs and phytol were quantified using an external standard (1 mg of C22:0 in hexane); qualitative analysis was performed using a gas chromatography–mass spectrometer (TSQ 8000 EVO GC-MS; Thermo Fisher Scientific, Waltham, MA, USA) and reconfirmed using authentic standards (Supelco 37 Component FAME Mix and phytol; Sigma-Aldrich, St. Louis, MO, USA). The content (w w^{-1}, %) and yield (mg L^{-1}) were summed and expressed in terms of milligrams of FAMEs (or phytol) per gram of dry cell weight (DCW) and milligrams of FAMEs (or phytol) per liter of culture volume.

Statistical tests

Results with a p-value < 0.05 were considered statistically significant. The optimization values of significant medium components were calculated using the Minitab software ver. 14 (Minitab Inc., State College, PA, USA) and linear multiple regression was used for the statistical analysis.

RESULTS AND DISCUSSION

Component selection

To eliminate unnecessary or negative elements of the
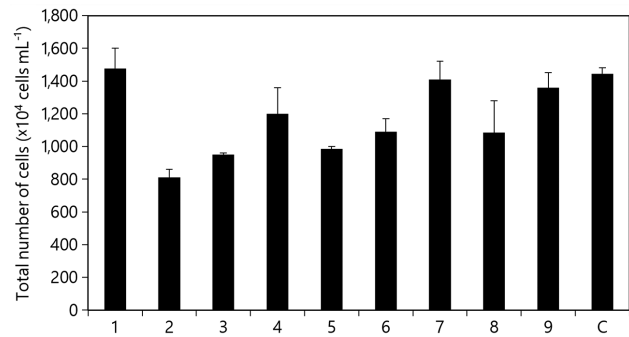

Fig. 1. Elimination test results for KSF0031. Effect of each component on cell growth. Total cell numbers in the absence of 1, NaNO₃; 2, K₂HPO₄; 3, MgSO₄·7H₂O; 4, CaCl₂·2H₂O; 5, citric acid; 6, ammonium ferric citrate green; 7, EDTA·Na₂; 8, Na₂CO₃; 9, trace metals; C, control (no absence). Data shown represent the average cell densities ± standard deviation from triplicates (n = 3).

microalgal medium, all nine components were analyzed individually (Fig. 1). In the elimination test to optimize the culture of KSF0031, we found five significant factors among the medium components, namely K₂HPO₄, MgSO₄·7H₂O, citric acid, AFCg, and Na₂CO₃, all of which had positive effects. In each medium, when any one of these five components were removed, the growth of KSF0031 was restricted compared to that observed upon using the original BG-11 medium. The non-significant factors were NaNO₃, CaCl₂·2H₂O, EDTA·Na₂, and trace metals. In each medium, when any of these four components were removed, the growth of KSF0031 was not significantly affected when compared to that observed upon using the original BG-11 medium (Fig. 1).

Screening of components using the Placket-Burman design

To select the component having optimal effects on KSF0031 cell numbers, the five components showing positive effects were tested using the Plackett-Burman design. Table 1 lists the test values, effects, t-statistics, and p-values. Results with a p-value lower than 0.05 were treated as showing a significant effect on the growth of KSF0031. NaNO₃, CaCl₂·2H₂O, EDTA·Na₂, and trace metals were not significant factors (p > 0.05) (Table 1). The remaining components (K₂HPO₄, MgSO₄·7H₂O, citric acid, AFCg, and Na₂CO₃) were significant (p < 0.05). These components were re-analyzed using a secondary Plackett-Burman design. Ten media, in each of which the concentrations were adjusted to -value (mM) and +value (mM), were prepared for the component analysis corresponding to the five significant variables (Table 2). Cell

growth was measured in media adjusted to each concentration. Experiments were performed by varying the concentration range (0.2 times [-], 1.1 times [0], and 2 times [+] of the original concentration of BG-11) of the significant factors obtained through the elimination test, and the number of cells was measured. Three components showed significant effects, where two components, K_2HPO_4 and $MgSO_4 \cdot 7H_2O$, exhibited positive effects; AFCg exhibited a negative effect (Table 2).

Optimization of medium components for KSF0031 growth

The Box-Behnken design was performed based on the statistical results of the Plackett-Burman design of KSF0031. It was applied to measure the interdependence of three component variables, K_2HPO_4 (X_2), $MgSO_4 \cdot 7H_2O$ (X_3), and AFCg (X_6), in their effects on cell biomass. For positive effect factors, (+) was set as twice the original

Table 1. Statistical analysis of medium component using the initial Plackett-Burman test

Variable	Component	-value (mM)	+value (mM)	Effect	T statistics	p-value
X_1	$NaNO_3$	0	17.6	360	1.69	0.102
X_2	K_2HPO_4	0	0.23	1,077.5	5.05	<0.001
X_3	$MgSO_4 \cdot 7H_2O$	0	0.3	970	4.55	<0.001
X_4	$CaCl_2 \cdot 2H_2O$	0	0.24	295	1.38	0.177
X_5	Citric acid	0	0.031	595	2.79	0.009
X_6	AFCg	0	0.021	457.5	2.14	0.040
X_7	$EDTA \cdot Na_2$	0	0.0027	147.5	0.69	0.495
X_8	Na_2CO_3	0	0.19	490	2.30	0.029
X_9	Trace metals	0	0.058	397.5	1.86	0.072

AFCg, ammonium ferric citrate green.

Table 2. Statistical analysis of selected medium components using the secondary Plackett-Burman design

Variable	Component	-value (mM)	+value (mM)	Effect	T statistics	p-value
X_2	K_2HPO_4	0.046	0.46	563.7	6.83	<0.001
X_3	$MgSO_4 \cdot 7H_2O$	0.06	0.6	384.6	4.66	<0.001
X_5	Citric acid	0.0062	0.062	-27.9	-0.34	0.739
X_6	AFCg	0.0042	0.042	-437.1	-5.30	<0.001
X_8	Na_2CO_3	0.038	0.38	-45.4	-0.55	0.588

AFCg, ammonium ferric citrate green.

Table 3. Box-Behnken optimization of selected significant medium components

Variable	Medium component	-value (mM)	0 value (mM)	+value (mM)
X_2	K_2HPO_4	0.046	0.253	0.46
X_3	$MgSO_4 \cdot 7H_2O$	0.06	0.33	0.6
X_6	AFCg	0.0021	0.01155	0.021

AFCg, ammonium ferric citrate green.

Table 4. Response surface regression for selected medium components using Box-Behnken design

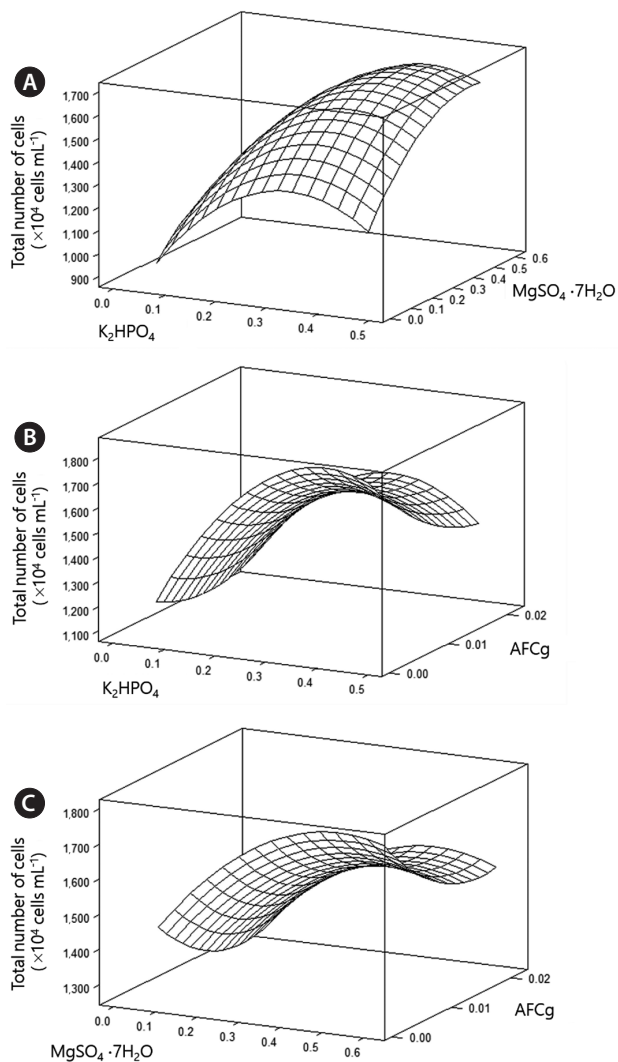| Variable	Component	Coefficient	T statistics	p-value
Constant		1,568.3	22.248	<0.001
X_2	K_2HPO_4	190.6	4.416	0.007
X_3	$MgSO_4 \cdot 7H_2O$	136.9	3.171	0.025
X_6	AFCg	-91.5	-2.120	0.088
X_2^2		-240.2	-3.780	0.013
X_3^2		-127.7	-2.009	0.101
X_6^2		75.1	1.182	0.290
X_2X_3		66.0	1.081	0.329
X_2X_6		-103.8	-1.699	0.150
X_3X_6		-19.7	-0.324	0.759

AFCg, ammonium ferric citrate green.

Fig. 2. Three-dimensional response plots showing the effects of K_2HPO_4 and $MgSO_4 \cdot 7H_2O$ (A), K_2HPO_4 and ammonium ferric citrate green (AFCg) (B), and $MgSO_4 \cdot 7H_2O$ and AFCg (C).
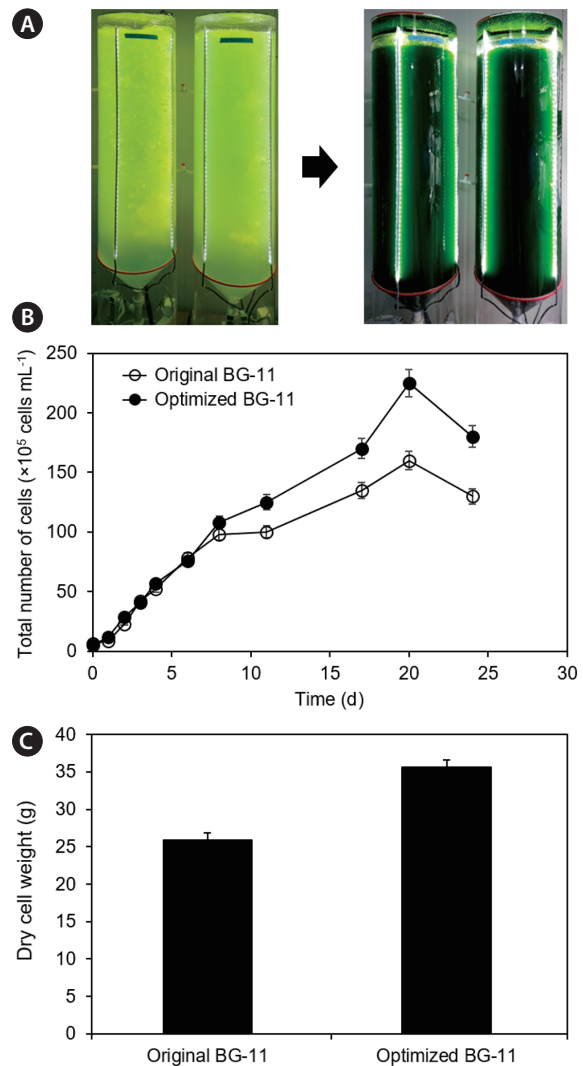

Fig. 3. Comparison of cell growth and biomass of KSF0031 in different conditions in 100-L culture. (A) 100-L photobioreactor for 1 d (left) and 24 d (right). (B) Time profile of KSF0031 cell growth. The open and solid circles represent the original and optimized BG-11 conditions, respectively. (C) Cell weights with moisture removed. Data are represented as mean ± standard deviation of duplicates (n = 2).

concentration (mM) of BG-11 medium, and (-) was set as 1/10 of (+). For negative effect factors, (+) was set as the original concentration (mM) and (-) was set as 1/10 of (+). Other factors ($NaNO_3$, $CaCl_2 \cdot 2H_2O$, citric acid, $EDTA \cdot Na_2$, Na_2CO_3, and trace metals) were added at their original concentrations (mM) (Table 3).

The optimization values were calculated (Table 3). The estimated coefficients, t-statistics, and p-values were also calculated (Table 4). The effects of the other three variables at different levels are shown in Fig. 2. The expected number of KSF0031 cells was calculated using the Minitab software and determined to be 1.90×10^7 cells mL^{-1} with optimized concentrations of K_2HPO_4, $MgSO_4 \cdot 7H_2O$, and AFCg as 0.4, 0.55, and 0.0021 mM, respectively. The final

composition was as follows (mM): $NaNO_3$, 17.6; K_2HPO_4, 0.4; $MgSO_4 \cdot 7H_2O$, 0.55; $CaCl_2 \cdot 2H_2O$, 0.24; citric acid, 0.031; AFCg, 0.0021; $EDTA \cdot Na_2$, 0.0027; Na_2CO_3, 0.19; and trace metals, 0.058 (Table 5).

Comparison of KSF0031 growth, and lipid and phytol production in the original medium vs. optimized medium

The growth of KSF0031 and its production of lipids and phytol in the medium optimized via the Box-Behnken design were analyzed. Fig. 3B shows the number of KSF0031

cells mL^{-1} in 100 L BG-11 culture media for 24 d. Maximal concentrations of $(160 \pm 8) \times 10^5$ and $(225 \pm 11) \times 10^5$ cells mL^{-1} were obtained in the original and optimized BG-11 medium, respectively. The dry mass of harvested cells cultivated in the optimized BG-11 medium was 35.60 ± 1 g, which constituted a 37.5% improvement in biomass when compared with the dry mass of KSF0031 cells from the original BG-11 medium (Fig. 3C). Although the levels of the two components were elevated in the optimized medium, the production cost of KSF0031 in this medium could be significantly reduced (Supplementary Table S1). The biomass of KSF0031 was increased in the optimized medium where the concentration of the negative factor AFCg was reduced by 10 fold. This gain was due to relief from iron toxicity effects on the cells. Iron, which can be considered a heavy metal, plays an important role in metabolism at low concentrations but can be toxic to microalgal cells at high concentrations (Subramaniyam et al. 2016). Through statistical optimization, it is possible to determine the appropriate concentration of heavy metal ions (Jaafari and Yaghmaeian 2019). After cultivation for 24 d in the original and optimized media, lipids were extracted from the dried biomass to obtain FAMEs and phytol. The PUFA content in the total fatty acids of *Micractinium reisseri* was 66% (Abou-Shanab et al. 2014). The PUFA content of *Micractinium singularis* reported in 2020 was 55.5% (Jo et al. 2020). There was no information on PUFA production (mg g^{-1} DCW) reported in either of these studies. In a study with *M. reisseri* reported in 2019, only 0.54 mg g^{-1} DCW of PUFA was produced (Elshobary et al. 2019). Reports on PUFA and phytol production in *Micractinium* species are limited, and research on the applications of *Micractinium* sp. is in its infancy. To evaluate the production of PUFAs and phytol, gas chromatography analysis was performed (Fig. 4, Supplementary Fig. S2). The dominant fatty acids of KSF0031 were linolenic acid
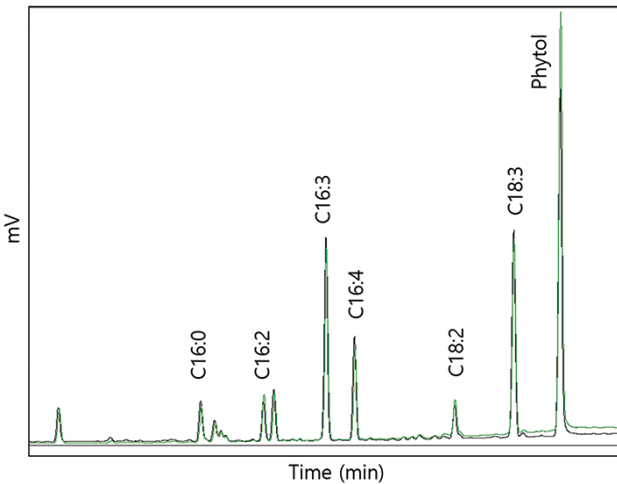

Fig. 4. Gas chromatography results showing the fatty acid methyl esters and phytol on extracts of *Micractinium variabile* KSF0031. Chromatograph peak: black line, extract in original BG-11; green line, extract in optimized BG-11 on KSF0031.

Table 5. Comparison of medium composition of original BG-11 and optimized BG-11

Component	Original BG-11 (mM)	Optimized BG-11 (mM)
NaNO$_3$	17.60	17.60
K$_2$HPO$_4$	0.23	0.40
MgSO$_4$·7H$_2$O	0.30	0.55
CaCl$_2$·2H$_2$O	0.24	0.24
Citric acid	0.031	0.031
AFCg	0.021	0.0021
EDTA·Na$_2$	0.0027	0.0027
Na$_2$CO$_3$	0.19	0.19
Trace metals	0.058	0.058

AFCg, ammonium ferric citrate green.

(C18:3) and hexadecatrienoic acid (C16:3). Sorokina et al. (2020) reported that the dominant fatty acids in *Micractinium* sp. IC-44 were C16:0 and C18:2 when cultured in

Table 6. Content and yield of FAMEs and phytol from KSF0031

Fatty acid (%, w/w)	Original BG-11		Optimized BG-11	
	Content (%)	Yield (mg g^{-1} DCW)	Content (%)	Yield (mg g^{-1} DCW)
Palmitic acid (C16:0)	3.56	0.79	3	0.83
Hexadecadienoic acid (C16:2)	3.36	0.75	3.68	1.01
Hexadecatrienoic acid (C16:3)	17.27	3.83	15.48	4.26
Hexadecatetraenoic acid (C16:4)	8.78	1.95	7.04	1.94
Linoleic acid (C18:2)	4.24	0.94	4.36	1.2
Linolenic acid (C18:3)	18.76	4.16	16.79	4.62
Phytol	33.29	7.38	39.95	10.98
Unknown	10.73	2.38	9.71	2.67
Total	100	22.17	100	27.51

FAME, fatty acid methyl esters; DCW, dry cell weight.

Bold's basal medium at 28°C. Although the two strains belong to the same genus, KSF0031 is a psychrotrophic microalga in Antarctica, which has the characteristic of producing more PUFAs (Teoh et al. 2004). Our data indicate that compared to the original BG-11, using the optimized BG-11 medium leads to higher FAME and phytol production values (13.03 and 10.98 mg g^{-1} DCW, representing 12.04 and 48.78% yield increases, respectively) (Table 6). Phytol-producing microalgal strains have rarely been reported; the phytol contents of the ethanol extracts of *Porphyridium cruentum*, *Phaeodactylum tricornutum*, and *Chlorella vulgaris* were 3.1, 8.4, and 5.5%, respectively (Rodriguez-Garcia and Guil-Guerrero 2008). There have been no studies on phytol production using polar microalgae, and here, we performed an optimized medium design for the first time. The Antarctic microalga KSF0031 showed a high phytol content of 33.29% of total fatty acids, and we were able to improve the phytol content to 39.95% by using optimized BG-11 medium.

CONCLUSION

Here, we reported the production of phytol and PUFAs as bioactive compounds in the Antarctic microalga *Micractinium variabile* KSF0031 for the first time; further, we optimized their production. To enhance the biomass productivity of KSF0031, we statistically optimized the medium components using the Plackett-Burman and Box-Behnken designs. When AFCg, a component that had a negative effect, was diminished and K_2HPO_4 and $MgSO_4 \cdot 7H_2O$, components that had a positive effect, were elevated, the biomass production of KSF0031 was increased. In this study, a 37.5% increase in biomass production was obtained using a sequential statistical method. The use of the optimized medium was shown to reduce the production cost of KSF0031. In addition, we obtained 12.04% and 48.78% improved PUFA and phytol levels, respectively, in the optimized BG-11 medium. Because this Antarctic microalga could be a potential resource in the biomedical industry, the medium designed in this study may play an important role in improving the production of cell biomass and bioactive ingredients.

ACKNOWLEDGEMENTS

CONFLICTS OF INTEREST

The authors declare that they have no potential conflicts of interest.

SUPPLEMENTARY MATERIALS

Supplementary Table S1. Comparison of costs of media used for the biomass production of KSF0031 (https://www.e-algae.org).

Supplementary Fig. S1. Effect of temperature on the growth of *Micractinium variabile* KSF0031 (https://www.e-algae.org).

Supplementary Fig. S2. Gas chromatography mass spectrometry results showing the fatty acid methyl esters and phytol with extracts of *Micractinium variabile* KSF0031 (https://www.e-algae.org).

REFERENCES

Abou-Shanab, R. A. I., El-Dalatony, M. M., El-Sheekh, M. M., Ji, M. -K., Salama, E. -S., Kabra, A. N. & Jeon, B. -H. 2014. Cultivation of a new microalga, *Micractinium reisseri*, in municipal wastewater for nutrient removal, biomass, lipid, and fatty acid production. Biotechnol. Bioprocess Eng. 19:510–518.

Barker, P. F., Filippelli, G. M., Florindo, F., Martin, E. E. & Scher, H. D. 2007. Onset and role of the Antarctic Circumpolar Current. Deep Sea Res. Part II Top. Stud. Oceanogr. 54:2388–2398.

Borchert, E., Jackson, S. A., O'Gara, F. & Dobson, A. D. W. 2017. Psychrophiles as a source of novel antimicrobials. *In* Margesin, R. (Ed.) *Psychrophiles: from Biodiversity to Biotechnology*. Springer, Cham, pp. 527–540.

Box, G. E. P. & Behnken, D. W. 1960. Some new three level designs for the study of quantitative variables. Technometrics 2:455–475.

Brouchkov, A., Melnikov, V., Kalenova, L., Fursova, O., Pogorelko, G., Potapov, V., Fursova, N., Ignatov, S., Brenner, E., Bezrukov, V. & Muradian, K. 2017. Permafrost bacteria in biotechnology: biomedical applications. *In* Margesin, R. (Ed.) *Psychrophiles: from Biodiversity to Biotechnology*. Springer, Cham, pp. 541–554.

Chae, H., Lim, S., Kim, H. S., Choi, H. -G. & Kim, J. H. 2019. Morphology and phylogenetic relationships of *Micractinium* (Chlorellaceae, Trebouxiophyceae) taxa, including three new species from Antarctica. Algae 34:267–275.

Cho, S. M., Kim, S., Cho, H., Lee, H., Lee, J. H., Lee, H., Park,

H., Kang, S., Choi, H. -G. & Lee, J. 2019. Type II ice-binding proteins isolated from an arctic microalga are similar to adhesin-like proteins and increase freezing tolerance in transgenic plants. Plant Cell Physiol. 60:2744–2757.

Chowdhury, R. R., Fitch, R. W. & Ghosh, S. K. 2013. Efficacy of phytol-derived diterpenoid immunoadjuvants over alum in shaping the murine host's immune response to *Staphylococcus aureus*. Vaccine 31:1178–1186.

Czyrski, A. & Sznura, J. 2019. The application of Box-Behnken-Design in the optimization of HPLC separation of fluoroquinolones. Sci. Rep. 9:19458.

Ekpenyong, M. G., Antai, S. P., Asitok, A. D. & Ekpo, B. O. 2017. Plackett-Burman design and response surface optimization of medium trace nutrients for glycolipopeptide biosurfactant production. Iran. Biomed. J. 21:249–260.

Elshobary, M. E., Abo-Shady, A. M., Khairy, H. M., Essa, D., Zabed, H. M., Qi, X. & Abomohra, A. E. -F. 2019. Influence of nutrient supplementation and starvation conditions on the biomass and lipid productivities of *Micractinium reisseri* grown in wastewater for biodiesel production. J. Environ. Manage. 250:109529.

Ghaneian, M. T., Ehrampoush, M. H., Jebali, A., Hekmatimoghaddam, S. & Mahmoudi, M. 2015. Antimicrobial activity, toxicity and stability of phytol as a novel surface disinfectant. Environ. Health Eng. Manag. J. 2:13–16.

Gutiérrez, S., Svahn, S. L. & Johansson, M. E. 2019. Effects of omega-3 fatty acids on immune cells. Int. J. Mol. Sci. 20:5028.

Islam, M. T., de Alencar, M. V. O. B., da Conceição Machado, K., da Conceição Machado, K., de Carvalho Melo-Cavalcante, A. A., de Sousa, D. P. & de Freitas, R. M. 2015. Phytol in a pharma-medico-stance. Chem. Biol. Interact. 240:60–73.

Jaafari, J. & Yaghmaeian, K. 2019. Optimization of heavy metal biosorption onto freshwater algae (*Chlorella coloniales*) using response surface methodology (RSM). Chemosphere 217:447–455.

Jo, S. -W., Kang, N. -S., Chae, H., Lee, J. A., Kim, K. M., Yoon, M., Hong, J. W. & Yoon, H. -S. 2020. First record of a marine microalgal species, *Micractinium singularis* (Trebouxiophyceae) isolated from Janghang Harbor, Korea. Korean J. Environ. Biol. 38:61–70.

Khan, M. I., Shin, J. H. & Kim, J. D. 2018. The promising future of microalgae: current status, challenges, and optimization of a sustainable and renewable industry for biofuels, feed, and other products. Microb. Cell Fact. 17:36.

Kim, E. J., Jung, W., Lim, S., Kim, S., Han, S. J. & Choi, H. -G. 2016. Growth and lipid content at low temperature of Arctic alga *Chlamydomonas* sp. KNM0029C. Bioprocess Biosyst. Eng. 39:151–157.

Kim, E. J., Lee, J. H., Lee, S. G. & Han, S. J. 2017. Improving thermal hysteresis activity of antifreeze protein from recombinant *Pichia pastoris* by removal of N-glycosylation. Prep. Biochem. Biotechnol. 47:299–304.

Komiya, T., Kyohkon, M., Ohwaki, S., Eto, J., Katsuzaki, H., Imai, K., Kataoka, T., Yoshioka, K., Ishii, Y. & Hibasami, H. 1999. Phytol induces programmed cell death in human lymphoid leukemia Molt 4B cells. Int. J. Mol. Med. 4:377–380.

Murbach Teles Andrade, B. F., Nunes Barbosa, L., da Silva Probst, I. & Fernandes Júnior, A. 2014. Antimicrobial activity of essential oils. J. Essent. Oil Res. 26:34–40.

Park, H. J., Lee, C. W., Kim, D., Do, H., Han, S. J., Kim, J. E., Koo, B. -H., Lee, J. H. & Yim, J. H. 2018. Crystal structure of a cold-active protease (Pro21717) from the psychrophilic bacterium, *Pseudoalteromonas arctica* PAMC 21717, at 1.4 Å resolution: structural adaptations to cold and functional analysis of a laundry detergent enzyme. PLoS ONE 13:e0191740.

Plackett, R. L. & Burman, J. P. 1946. The design of optimum multifactorial experiments. Biometrika 33:305–325.

Prabuseenivasan, S., Jayakumar, M. & Ignacimuthu, S. 2006. *In vitro* antibacterial activity of some plant essential oils. BMC Complement. Alternat. Med. 6:39.

Remize, M., Brunel, Y., Silva, J. L., Berthon, J. -Y. & Filaire, E. 2021. Microalgae n-3 PUFAs production and use in food and feed industries. Mar. Drugs 19:113.

Rodriguez-Garcia, I. & Guil-Guerrero, J. L. 2008. Evaluation of the antioxidant activity of three microalgal species for use as dietary supplements and in the preservation of foods. Food Chem. 108:1023–1026.

Siram, K., Rahman, S. M. H., Balakumar, K., Duganath, N., Chandrasekar, R. & Hariprasad, R. 2019. Pharmaceutical nanotechnology: brief perspective on lipid drug delivery and its current scenario. *In* Andrew, W. (Ed.) *Biomedical Applications of Nanoparticles*. William Andrew Publishing, New York, pp. 91–115.

Sorokina, K. N., Samoylova, Y. V., Gromov, N. V., Ogorodnikova, O. L. & Parmon, V. N. 2020. Production of biodiesel and succinic acid from the biomass of the microalga *Micractinium* sp. IC-44. Bioresour. Technol. 317:124026.

Stanier, R. Y., Kunisawa, R., Mandel, M. & Cohen-Bazire, G. 1971. Purification and properties of unicellular blue-green algae (order Chroococcales). Bacteriol. Rev. 35: 171–205.

Subramaniyam, V., Subashchandrabose, S. R., Thavamani, P., Chen, Z., Krishnamurti, G. S. R., Naidu, R. & Megharaj, M. 2016. Toxicity and bioaccumulation of iron in soil microalgae. J. Appl. Phycol. 28:2767–2776.

Suh, S. -S., Hong, J. -M., Kim, E. J., Jung, S. W., Chae, H.,

Kim, J. E., Jim, J. H., Kim, I. -C. & Kim, S. 2019. Antarctic freshwater microalga, *Chloromonas reticulata*, suppresses inflammation and carcinogenesis. Int. J. Med. Sci. 16:189–197.

Suh, S. -S., Hong, J. -M., Kim, E. J., Jung, S. W., Kim, S. -M., Kim, J. E., Kim, I. -C. & Kim, S. 2018. Anti-inflammation and anti-cancer activity of ethanol extract of antarctic freshwater microalga, *Micractinium* sp. Int. J. Med. Sci. 15:929–936.

Teoh, M. -L., Chu, W. -L., Marchant, H. & Phang, S. -M. 2004. Influence of culture temperature on the growth, biochemical composition and fatty acid profiles of six Antarctic microalgae. J. Appl. Phycol. 16:421–430.